Anisotropic Magnetic Responses of Topological Crystalline Superconductors

Yuansen Xiong [1], Ai Yamakage [1,2,*], Shingo Kobayashi [1,2], Masatoshi Sato [3] and Yukio Tanaka [1]

[1] Department of Applied Physics, Nagoya University, Nagoya 464-8603, Japan;
    yuu@rover.nuap.nagoya-u.ac.jp (Y.X.); shingo@rover.nuap.nagoya-u.ac.jp (S.K.);
    ytanaka@nuap.nagoya-u.ac.jp (Y.T.)
[2] Institute for Advanced Research, Nagoya University, Nagoya 464-8601, Japan
[3] Yukawa Institute for Theoretical Physics, Kyoto University, Kitashirakawa Oiwake-Cho,
    Kyoto 606-8502, Japan; msato@yukawa.kyoto-u.ac.jp
*   Correspondence: ai@rover.nuap.nagoya-u.ac.jp; Tel.: +81-52-789-3701

Abstract: Majorana Kramers pairs emerged on surfaces of time-reversal-invariant topological crystalline superconductors show the Ising anisotropy to an applied magnetic field. We clarify that crystalline symmetry uniquely determines the direction of the Majorana Ising spin for given irreducible representations of pair potential, deriving constraints to topological invariants. In addition, necessary conditions for nontrivial topological invariants protected by the *n*-fold rotational symmetry are shown.

1. Introduction

Topological superconductors are fully or partially gapped systems hosting gapless states on their surfaces [1–4] as Andreev bound states [5–8]. The gapless surface states behave as Majorana fermions, which are self-conjugate particles and protected by the topological invariant associated to (broken) symmetries. Due to the stability and the so-called non-Abelian statistics derived from the self-conjugate property, one would expect that topological superconductors can be a platform of the fault-tolerant topological quantum computation [9].

For further achievement, it is necessary to detect and manipulate the Majorana fermions. Applying an external magnetic field is a one way to destruct Majorana fermions in time-reversal-invariant (DIII [10–12]) topological superconductors since a magnetic field breaks time-reversal symmetry. However, Majorana fermions still remain gapless when an applied magnetic field is normal to a certain direction. Namely, Majorana fermions exhibit the Ising anisotropy [13–22]. In this sense, Majorana fermions are referred to as Majorana Ising spin.

Shiozaki and Sato [23] have unveiled that the underlying mechanism of Majorana Ising spin is the protection by crystalline symmetry, i.e., an extension from topological crystalline superconductivity [24–27]. In this paper, we develop the theory and find that the direction of Majorana Ising spin is uniquely determined for a given irreducible representation [28,29] of the pair potential. The obtained result can be applied to all the space groups hence we believe that it is useful for studies on topological-superconductor materials and experiments.

The paper is organized as follows. We start with a brief review on Majorana Ising spin in Section 2 and clearly summarize issues to be addressed. We derive conditions for nontrivial topological invariant in Section 3 in systems with time-reversal and crystalline symmetries. From the obtained conditions, one finds the direction of Majorana Ising spin and summarizes it in tables (Appendix C).

Besides Majorana Ising spin, in Section 4, we also derive the winding number corresponding to the surface Majorana fermions protected by *n*-fold rotational symmetry, in a manner similar to that in Section 3. An example of the application of our general theory is shown in Section 5. We finally summarize the paper in Section 6.

2. Preliminary

Before going into the main discussion, we first review zero-energy states and the associated topological invariants in superconductors. A BdG Hamiltonian $H(k)$ has the form

$$H(k) = \begin{pmatrix} h(k) - \mu & \Delta(k) \\ \Delta(k) & -h(k) + \mu \end{pmatrix} = [h(k) - \mu]\,\tau_z + \Delta(k)\tau_x, \tag{1}$$

in the basis of $(c_\uparrow(k), c_\downarrow(k), c_\uparrow^\dagger(-k), -c_\uparrow^\dagger(-k))$, where $\uparrow$ and $\downarrow$ denote the spin up and down, respectively, and the spin indices in $h(k)$ and $\Delta(k)$ are implicit. Note that one can choose $\Delta(k) = \Delta(k)^\dagger$ for time-reversal-invariant superconductors. The Hamiltonian preserves time-reversal T symmetry

$$h(k) = T^{-1}h(-k)T, \ \Delta(k) = T^{-1}\Delta(-k)T, \ H(k) = \mathcal{T}^{-1}H(-k)\mathcal{T}, \ \mathcal{T} = \tau_0 T, \tag{2}$$
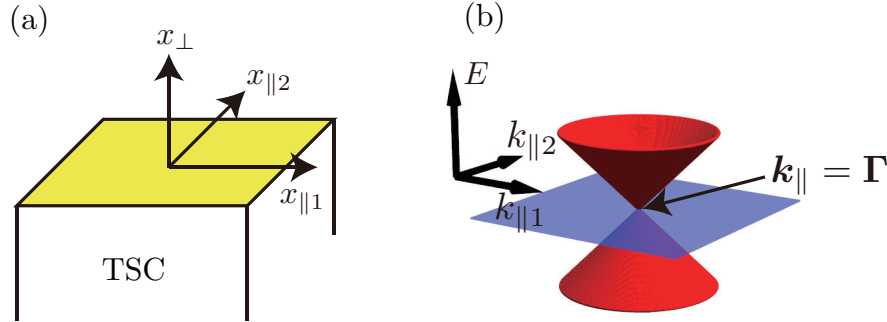
and particle-hole $\mathcal{C}$ symmetry

$$H(k) = -\mathcal{C}^{-1}H(-k)\mathcal{C}, \ \mathcal{C} = \tau_y \mathcal{T}. \tag{3}$$

Combining these symmetries, chiral symmetry holds;

$$\{\Gamma, H(k)\} = 0, \ \Gamma = \mathcal{C}\mathcal{T} = \tau_y. \tag{4}$$

Next, we introduce the topological invariant corresponding to the number of zero-energy states on the surface, which are located on $x_\perp = 0$ (Figure 1a).

Figure 1. (**a**) Topological superconductor (TSC) with the surface on $x_\perp = 0$; (**b**) Energy dispersion of the surface Majorana zero modes located at the time-reversal-invariant momentum $k_\parallel = \Gamma$.

The time-reversal-invariant momentum at which the zero-energy states appear is set to $k_\parallel = \Gamma$ (Figure 1b). The one-dimensional topological invariant W [30] is given by

$$W = \frac{i}{4\pi} \int_{-\pi/a_\perp}^{\pi/a_\perp} dk_\perp \mathrm{tr}\left[\Gamma H(k_\perp)^{-1}\frac{\partial H(k_\perp)}{\partial k_\perp}\right]_{k_\parallel = \Gamma} \in \mathbb{Z}, \ H(k_\perp) = H(k)|_{k_\parallel = \Gamma}, \tag{5}$$

where $H(k_\perp) = H(k_\perp + 2\pi/a_\perp)$. This invariant is equal to the number of the zero-energy surface states (see Appendix A). In time-reversal-invariant spinful systems, however, the above topological invariant always vanishes owing to time-reversal symmetry [10–12,31], which requires $\{\mathcal{T}, \Gamma\} = 0$ and

$$
\begin{aligned}
W^* &= \frac{-i}{4\pi} \int_{-\pi/a_\perp}^{\pi/a_\perp} dk_\perp \, \mathrm{tr} \left[\Gamma^* H(k_\perp)^{*-1} \frac{\partial H(k_\perp)^*}{\partial k_\perp} \right] \\
&= \frac{-i}{4\pi} \int_{-\pi/a_\perp}^{\pi/a_\perp} dk_\perp \, \mathrm{tr} \left[(-\Gamma) H(-k_\perp)^{-1} \frac{\partial H(-k_\perp)}{\partial k_\perp} \right] = -W,
\end{aligned}
\tag{6}
$$

using $\mathcal{T} H(\boldsymbol{k}) \mathcal{T}^{-1} = H(-\boldsymbol{k})$, hence $W = 0$.

The topological invariant can take a finite value with the help of an order-2 symmetry operation U that involves the spin and respects the surface: $[U, H(k_\perp)] = 0$. Now we introduce a modified chiral operator Γ_U as

$$
\Gamma_U = e^{i\phi_U} U \Gamma, \ \Gamma_U^2 = 1,
\tag{7}
$$

where the phase ϕ_U is chosen to satisfy $\Gamma_U^2 = 1$. The modified topological invariant $W[U]$ is given by replacing Γ with Γ_U;

$$
W[U] = \frac{i}{4\pi} \int_{-\pi/a_\perp}^{\pi/a_\perp} dk_\perp \, \mathrm{tr} \left[\Gamma_U H(k_\perp)^{-1} \frac{\partial H(k_\perp)}{\partial k_\perp} \right],
\tag{8}
$$

which is free from the condition of Equation (6) when the following condition is satisfied;

$$
[\mathcal{T}, \Gamma_U] = 0.
\tag{9}
$$

Normally, order-2 symmetry operations stem from crystalline point/space-group symmetries such as two-fold rotations and reflections with respect to the $x_\perp$ axis. This means that systems with $W[U] \neq 0$ are interpreted as a one-dimensional topological crystalline superconductor.

In the last part of this section, we review that $W[U]$ naturally explains the Ising-anisotropic response to a magnetic field [21,23]. The symmetry operation U is taken to be a two-fold rotation or a reflection. The symmetry operation U flips or keeps the direction of applied magnetic field, i.e., $\{U, H_{\mathrm{mag}}\} = 0$ or $[U, H_{\mathrm{mag}}] = 0$, respectively. Here H_{mag} denotes the Hamiltonian of magnetic field including the Zeeman and vector potential terms. These operations are summarized in Table 1.

Table 1. Symmetry of magnetic field $\boldsymbol{B}$ applied along the $x_\perp$, $x_{\|1}$, and $x_{\|2}$ directions, which are depicted in Figure 1. $C_2(x_\perp)$ is the two-fold rotation along the $x_\perp$ axis. $\sigma(x_i x_j)$ is the mirror reflection with respect to the $x_i x_j$ plane. These are symmetry operations of the semi-infinite system with the surface of $x_\perp = 0$. $-$ (+) indicates that the magnetic field is (not) flipped by the symmetry operation. S denotes the direction of Majorana Ising spin protected by the topological invariant $W[U]$ for $U = C_2(x_\perp)$, $\sigma(x_\perp x_{\|1})$, and $\sigma(x_\perp x_{\|2})$.

U	$B \parallel x_\perp$	$B \parallel x_{\|1}$	$B \parallel x_{\|2}$	S
$C_2(x_\perp)$	+	−	−	$x_\perp$
$\sigma(x_\perp x_{\|1})$	−	−	+	$x_{\|2}$
$\sigma(x_\perp x_{\|2})$	−	+	−	$x_{\|1}$

In the former case ($\{U, H_{\mathrm{mag}}\} = 0$), since the modified chiral symmetry still remains $\{\Gamma_U, H_0 + H_{\mathrm{mag}}\} = 0$, the modified topological invariant $W[U]$ is well-defined and shares the same number as that in the absence of magnetic field as long as H_{mag} is small enough, while not in the latter case ($[U, H_{\mathrm{mag}}] = 0$). From Table 1, the latter case is realized only in the case that magnetic field is applied for a specific direction in each symmetry operation. Therefore, the zero-energy surface states protected

by $W[U]$ are annihilated only by the magnetic field along the specific direction. Namely, Majorana fermions on the surface acts as an Ising spin under a magnetic field.

In the following sections, developing the theory, we show only one winding number among $W[C_2(x_\perp)]$, $W[\sigma(x_\perp x_{\|1})]$, and $W[\sigma(x_\perp x_{\|2})]$ is possible to take a finite value for a given surface and an irreducible representation of pair potential, i.e., the anisotropy of magnetic response is uniquely determined, irrespective of the details of the system.

3. Topological Invariants for Irreducible Representations

We show that only one among three possible topological invariants $W[C_2(x_\perp)]$, $W[\sigma(x_\perp x_{\|1})]$, and $W[\sigma(x_\perp x_{\|2})]$ can become finite in a given superconducting pair potential. This is the decisive evidence of Majorana Ising spin.

3.1. Symmetry of Crystalline Systems Including a Surface

In crystalline systems, all the symmetry operations other than time reversal and particle-hole transformation are elements of a space group. Here we focus on the momentum line including the time-reversal-invariant momentum $k = \Gamma$ along which the one-dimensional topological invariant is defined. Symmetry operations respecting the $k = \Gamma$ point are (screw) rotation and (glide) reflection, which are classified into those preserving (type-I) and inverting (type-II) the surface of $x_\perp = 0$. The type-I symmetry operations are two-fold (screw) rotation $C_2(x_\perp)$ along the $x_\perp$ axis and mirror (glide) reflections $\sigma(x_\perp x_{\|1})$ with respect to $x_\perp x_{\|1}$ plane and $\sigma(x_\perp x_{\|2})$ with respect to $x_\perp x_{\|2}$ plane (Figure 2a). The type-II symmetry operations, on the other hand, are two (screw) rotations [$C_2(x_{\|1})$ and $C_2(x_{\|2})$] and one mirror (glide) reflection [$\sigma(x_{\|1}x_{\|2})$], as shown in Figure 2b. Afterwards, we denote a type-I operation by U_i then we have
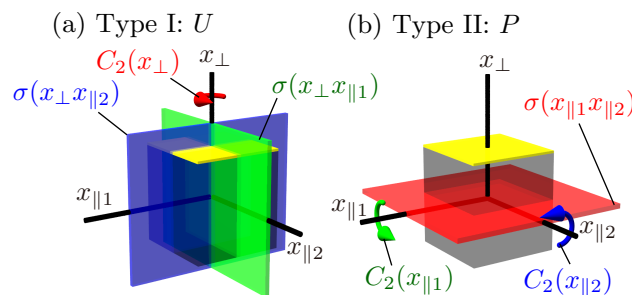
$$[U_i, h(k_\perp)] = 0. \tag{10}$$

The spatial inversion I is represented in terms of U_i as

$$I = U_i P_i, \tag{11}$$

for $i = 1, 2, 3$, where P_i is a type-II symmetry operation, i.e.,

$$h(k_\perp) = P_i^\dagger h(-k_\perp) P_i. \tag{12}$$

Figure 2. Point-group symmetry operations which preserve (**a**) and invert (**b**) the surface of $x_\perp = 0$.

3.2. Symmetry Operations in Superconducting States

Now define symmetry operations in a superconductor. A superconductor keeps a crystal symmetry S (U_i or P_i) where the pair potential $\Delta(k)$ is a one-dimensional representation of S;

$$\Delta(k) = \chi(S) S^\dagger \Delta(k') S, \tag{13}$$

where $\chi(S)$ is the character of the one-dimensional representation and $\boldsymbol{k}'$ is the momentum transformed by S. Then, the symmetry operation $\tilde{S}$ in the superconducting state is defined as

$$\tilde{S} = \begin{pmatrix} S & 0 \\ 0 & \chi(S)S \end{pmatrix}, \tag{14}$$

which satisfies $\tilde{S}^{\dagger}H(\boldsymbol{k})\tilde{S} = H(\boldsymbol{k}')$. If S obeys $S^2 \propto 1$, $\chi(S)$ of the one-dimensional representation is either $\chi(S) = 1$ or $\chi(S) = -1$, and

$$\tilde{S} = \begin{cases} S\tau_0, & \text{for } \chi(S) = +1, \\ S\tau_z, & \text{for } \chi(S) = -1. \end{cases} \tag{15}$$

In these cases, one obtains the following relation

$$\tilde{S}^{\dagger}\Gamma\tilde{S} = \chi(S)\Gamma, \tag{16}$$

for $\Gamma = \tau_y$ [see Equation (4)].

3.3. Topological Invariant

In the following, we derive necessary conditions for finite-valued topological invariants, which is defined by

$$W[\tilde{U}_i, \boldsymbol{x}_{\perp}] = \frac{i}{4\pi} \int_{\boldsymbol{k}\|\boldsymbol{x}_{\perp}} d\boldsymbol{k} \cdot \text{tr} \left[\Gamma_{\tilde{U}_i} H(\boldsymbol{k})^{-1} \frac{\partial H(\boldsymbol{k})}{\partial \boldsymbol{k}} \right]_{\boldsymbol{k}_{\|}=\Gamma}. \tag{17}$$

$\boldsymbol{x}_{\perp}$ indicates the direction normal to the surface, i.e., $W[\tilde{U}_i, \boldsymbol{x}_{\perp}]$ is the number of the Majorana zero modes on the surface perpendicular to $\boldsymbol{x}_{\perp}$. Note that the type-II symmetries P_i may define an topological invariant but it does not correspond to the zero-energy surface states since the surface is not invariant against P_i. This is why only the type-I symmetries U_i are considered here. Glide reflection along the direction parallel to the surface, e.g., a-glide with respect to the ac plane for the ab surface, is one of the possible type-I U_i symmetries for the winding number. Screw rotation, however, is not used for the winding number because the surface is not invariant by the operation. Glide reflection that translates a system along the direction normal to the surface and screw rotation may define a bulk invariant although the bulk-edge correspondence does not hold, as type-II P_i symmetry. Henceforth, for the rotational symmetries, we suppress the suffix $\boldsymbol{x}_{\perp}$ as $W[\tilde{C}_2(x_{\perp}), \boldsymbol{x}_{\perp}] = W[\tilde{C}_2(x_{\perp})]$, due to the uniqueness of the directions of the integrals, i.e., $\boldsymbol{x}_{\perp}$ must be along the rotational axis.

Now we derive the constraint to $W[\tilde{U}_i, \boldsymbol{x}_{\perp}]$ by the symmetries. One gets

$$W[\tilde{U}_i, \boldsymbol{x}_{\perp}] = +p(\tilde{U}_i, \tilde{U}_l)\chi(U_l)W[\tilde{U}_i, \boldsymbol{x}_{\perp}], \ W[\tilde{U}_i, \boldsymbol{x}_{\perp}] = -p(\tilde{U}_i, \tilde{P}_l)\chi(P_l)W[\tilde{U}_i, \boldsymbol{x}_{\perp}]. \tag{18}$$

These equations are derived by applying unitary transformations by $\tilde{U}_l$ and by $\tilde{P}_l$. Here we introduce $p(A, B)$ as

$$B^{-1}A\,B = p(A, B)A. \tag{19}$$

Note that $\tilde{U}_l$ includes the n-fold rotation (if exist) in addition to the two-fold rotations. In consequence, the conditions of

$$p(\tilde{U}_i, \tilde{U}_l)\chi(U_l) = -p(\tilde{U}_i, \tilde{P}_l)\chi(P_l) = 1, \tag{20}$$

and of $[\mathcal{T}, \Gamma_{\tilde{U}_i}] = 0$ (Equation (9)) are necessary for $W[\tilde{U}_i, \boldsymbol{x}_{\perp}] \neq 0$. From the above condition, $\chi(U_i) = 1$ is derived because of $p(U_i, U_i) = 1$.

Next, we prove that the two-fold symmorphic symmetry operations, rotations and reflections, satisfy the condition of Equation (9) while the nonsymmorphic ones, glide reflections, do not on the Brillouin zone boundary. Symmetry operations are represented by the direct product of real-space part O_i and spin part Σ_i, $U_i = O_i\Sigma_i$. For two-fold rotations and mirror reflections, the real-space part O_i is an orthogonal matrix with $O_i^2 = 1$ and $[O_i, \mathcal{T}] = 0$. The spin part is given by Pauli matrices then $\Sigma_i^\dagger = \Sigma_i$, $\Sigma_i^2 = 1$, and $\{\Sigma_i, \mathcal{T}\} = 0$. As a result, the chiral operator is given by $\Gamma_{\tilde{U}_i} = \tilde{U}_i\tau_y$ so that the condition of Equation (9) holds. For glide reflections, on the contrary, the orbital part O_i on the Brillouin zone boundary is purely-imaginary matrix hence the condition Equation (9) is not satisfied, i.e.,

$$W[\tilde{U}_i, x_\perp] = 0, \text{ for } k_\parallel \cdot \tau = \pm\pi/2, \tag{21}$$

with $\tilde{U}_i$ being a glide reflection, where τ is the translation vector of the glide reflection (for details, see Appendix B).

For symmorphic space groups, the necessary condition for $W[\tilde{U}_i, x_\perp] \neq 0$ is easily obtained as follows. The commutation relations of the representations for symmetry operations in a point group are uniquely determined to be

$$\{U_i, U_j\} = \{P_i, P_j\} = [U_i, P_i] = \{U_i, P_j\} = 0,\ i \neq j, \tag{22}$$

in spinful systems. With the help of the above relation, the condition Equation (20) reduces to

$$\chi(U_i) = -\chi(U_j) = -\chi(P_i) = \chi(P_j) = 1. \tag{23}$$

Here, $\chi(O)$ is the character of O hence the possible topological invariant is determined only from the representation theory of point group, irrespective of details of the system, as summarized in the tables in Appendix C. An example for a nonsymmorphic space group is also shown in Appendix C. The condition of $\chi(U_i)\chi(P_i) = \chi(U_iP_i) = -1$ is extracted from the above equations. This means that the character of the spatial inversion $I = U_iP_i$ must be -1 for the existence of topological superconductivity. That is consistent with the absence of time-reversal-invariant Majorana fermion in even-parity superconductors [32].

Finally, we show that two of $W[C_2(x_\perp)]$, $W[\sigma(x_\perp x_{\parallel 1})]$, and $W[\sigma(x_\perp x_{\parallel 2})]$ always vanish. Here $C_2(x_\perp)$ is the two-fold (not screw) rotation, $\sigma(x_\perp x_{\parallel j})$ is the mirror or glide reflection with respect to the $x_\perp x_{\parallel j}$ plane. The statement is immediately seen from Equation (23) for symmorphic space groups: $\chi(U_i) = 1$ and $\chi(U_j) = 1$ are not simultaneously satisfied. This is also true at $k_\parallel = 0$ for nonsymmorphic space groups since the commutation relations of symmetry operations are the same as those for the symmorphic space group. When $\sigma(x_\perp x_{\parallel 1})$ is the $x_{\parallel 1}$-glide reflection, the commutation relation changes from the symmorphic one at the boundary $k_{\parallel 1} = \pi/a_{\parallel 1}$. $W[\sigma(x_\perp x_{\parallel}1)]$, however, vanishes from Equation (21). In consequence, it is impossible that two of $W[C_2(x_\perp)]$, $W[\sigma(x_\perp x_{\parallel 1})]$, and $W[\sigma(x_\perp x_{\parallel 2})]$ simultaneously take nontrivial values.

4. Winding Number Protected by *n*-Fold Rotational Symmetry

Besides order-2 symmetries, we clarify the winding number protected by the *n*-fold ($n \geq 3$) rotational C_n symmetry, $[C_n, H(k)] = 0$. We derive the necessary condition for nonzero topological invariant associated with C_n for spinful systems. The spinless case was discussed in Ref. [33].

4.1. Definition

C_n is represented by $C_n = e^{-ij_z 2\pi/n}$, where j_z denotes the total angular momentum along the rotational axis. For spinful systems, $C_n^n = -1$ and the eigenvalue of C_n is obtained to be $e^{-i\mu 2\pi/n}$ for $\mu = 0, \cdots, n-1$. A Hamiltonian of C_n-symmetric system is block diagonalized to be

$$H(k) \rightarrow \text{diag}\left(H_0(k), \cdots, H_{n-1}(k)\right), \tag{24}$$

where $H_\mu(k) = V_\mu^\dagger H(k) V_\mu$, $V_\mu = (v_{\mu 1}, \cdots, v_{\mu g_\mu})$, $C_n v_{\mu j} = e^{-i\mu 2\pi/n} v_{\mu j}$, $C_n V_\mu = V_\mu e^{-i\mu 2\pi/n}$, is Hamiltonian in the $C_n = e^{-i\mu 2\pi/n}$ eigenspace. g_μ is the degeneracy of the eigenvalue of $e^{-i\mu 2\pi/n}$ then $\sum_{\mu=0}^{n-1} g_\mu = \dim H(k)$.

In a superconductor with the *n*-fold rotational symmetry, $[\tilde{C}_n, H(k)] = 0$, chiral symmetry in the eigenspaces is found when $[\Gamma, \tilde{C}_n] = 0$ holds:

$$\{\Gamma_\mu, H_\mu(k)\} = 0, \ \Gamma_\mu = V_\mu^\dagger \Gamma V_\mu, \ \Gamma_\mu^2 = 1. \tag{25}$$

Hereafter we assume that the pair potential is the *A* representation of C_n, i.e., $\Delta(\boldsymbol{k}) = C_n^\dagger \Delta(\boldsymbol{k'}) C_n$, because $[\Gamma, \tilde{C}_n] = 0$ holds only in this case. The winding number in each eigenspace is

$$W_\mu = \frac{i}{4\pi} \int_{-\pi/a_\perp}^{\pi/a_\perp} dk \, \text{tr} \left[\Gamma_\mu H_\mu(k)^{-1} \frac{\partial H_\mu(k)}{\partial k}\right], \tag{26}$$

which corresponds to the number of zero-energy end states of H_μ.

4.2. Time-Reversal Symmetry

Since the angular momentum is time-reversal odd, one finds

$$\mathcal{T}^{-1} \tilde{C}_n \mathcal{T} = \tilde{C}_n, \tag{27}$$

and

$$\mathcal{T} V_\mu = V_{-\mu} \mathcal{T}_{-\mu}, \ \mathcal{T}_\mu = V_\mu^\dagger \mathcal{T} V_{-\mu}. \tag{28}$$

T_μ is a unitary matrix:

$$[T_\mu T_\mu^\dagger]_{ij} = \sum_{k=1}^{g_{-\mu}} v_{\mu i}^\dagger \bar{v}_{-\mu k} \bar{v}_{-\mu k}^\dagger v_{\mu j} = \delta_{ij}, \tag{29}$$

where $\bar{v}_{\mu i}$ is defined by $\bar{v}_{\mu i} = \mathcal{T} v_{\mu i}$. These lead to

$$T_\mu^\dagger H_\mu(-k) T_\mu = +H_{-\mu}(k)^*, \ T_\mu^\dagger \Gamma_\mu T_\mu = -\Gamma_{-\mu}(k)^*. \tag{30}$$

As a result, one finds

$$W_\mu = \frac{i}{4\pi} \int_{-\pi/a_\perp}^{\pi/a_\perp} dk \, \text{tr} \left[-\Gamma_{-\mu}^* H_{-\mu}(-k)^{*-1} \frac{\partial H_{-\mu}(-k)^*}{\partial k}\right] = -W_{-\mu}^*, \tag{31}$$

by applying the unitary transform by T_μ. Thus, $W_\mu = -W_{-\mu}$ owing to W_μ is a real integer. This relation is a natural extension from Equation (6).

4.3. Spatial Symmetry

The commutation relation of C_n and spatial symmetries, U_l and P_l, is given by $[U_l, C_n] = 0$ for $[j_z, U_l] = 0$ and $U_l^\dagger C_n U_l = C_n^\dagger$ for $\{j_z, U_l\} = 0$. The same equations hold for P_l. This gives the transformation of Hamiltonian;

$$H_\mu(k) = U_{l,p(j_z,U_l)\mu}^\dagger H_{p(j_z,U_l)\mu}(k) U_{l,p(j_z,U_l)\mu}, \quad H_\mu(k) = P_{l,p(j_z,U_l)\mu}^\dagger H_{p(j_z,U_l)\mu}(-k) P_{l,p(j_z,U_l)\mu}, \tag{32}$$

where $U_{l,\mu} = V_\mu^\dagger U_l V_\mu$ and $P_{l,\mu} = V_\mu^\dagger P_l V_\mu$. The chiral operator is transformed by $U_{l,\mu}$ as

$$\Gamma_\mu = \chi(U_l) U_{l,p(j_z,U_l)}^\dagger \Gamma_{p(j_z,U_l)\mu} U_{l,p(j_z,U_l)}. \tag{33}$$

This is the same for $P_{l,\mu}$. The winding numbers satisfy the following relations;

$$W_\mu = \chi(U_l) W_{p(j_z,U_l)\mu} = -\chi(P_l) W_{p(j_z,P_l)\mu}. \tag{34}$$

Combining these and Equation (31), one finds a necessary condition

$$\chi(U_l) p(j_z, U_l) = -\chi(P_l) p(j_z, P_l) = 1, \tag{35}$$

for $W_\mu \neq 0$.

In symmorphic space groups, from the above conditions, W_μ takes a finite value only for the A_{1u} (or its compatible) representation. The (anti)commutation relations of j_z and the symmetry operations, $U_1 = C_n$, $U_2 = \sigma(x_\perp x_{\|1})$, $U_3 = \sigma(x_\perp x_{\|2})$, $P_1 = \sigma(x_{\|1} x_{\|2})$, $P_2 = C_2(x_{\|1})$, and $P_3 = C_2(x_{\|2})$, are given by

$$[j_z, C_n] = \{j_z, \sigma(x_\perp x_{\|1})\} = \{j_z, \sigma(x_\perp x_{\|2})\} = [j_z, \sigma(x_{\|1} x_{\|2})] = \{j_z, C_2(x_{\|1})\} = \{j_z, C_2(x_{\|2})\} = 0. \tag{36}$$

From this and Equation (35), the necessary condition is given by

$$\begin{aligned} \chi(C_n(x_\perp)) &= -\chi(\sigma(x_{\|1} x_{\|2})) = -\chi(\sigma(x_\perp x_{\|1})) = -\chi(\sigma(x_\perp x_{\|2})) \\ &= \chi(C_2(x_{\|1})) = \chi(C_2(x_\perp x_{\|2})) = 1. \end{aligned} \tag{37}$$

This holds for the A_{1u} representation of the pair potential.

5. Example: Bilayer Rashba System

As an example, we show the magnetic response of Majorana Ising spin in the bilayer Rashba superconductor [34], which are depicted in Figure 3. The Hamiltonian in the normal state reads

$$\mathcal{H}_0(k_x, k_y) = \frac{k_x^2 + k_y^2}{2m} \sigma_0 s_0 - \varepsilon \sigma_x s_0 + \alpha(k_x s_y - k_y s_x) \sigma_z, \tag{38}$$

where s and σ denote the Pauli matrices representing the spin and layer degrees of freedom, respectively. Time-reversal-invariant Bogoliubov-de Gennes (BdG) Hamiltonian has the form

$$\mathcal{H}_{\text{BdG}}(k_x, k_y) = \begin{pmatrix} \mathcal{H}_0(k_x, k_y) - \mu & \Delta(k_x, k_y) \\ \Delta(k_x, k_y) & -[\mathcal{H}_0(k_x, k_y) - \mu] \end{pmatrix} = [\mathcal{H}_0(k_x, k_y) - \mu]\tau_z + \Delta(k_x, k_y)\tau_x, \tag{39}$$

in the basis of $(c_{k\uparrow}, c_{k\downarrow}, c_{-k\downarrow}^\dagger, -c_{-k\uparrow}^\dagger)$, where the arrows $\uparrow$ and $\downarrow$ denote the up and down spins, respectively, and the indices for the layer degrees of freedom are implicit. When the Fermi level

μ is located within the hybridization gap, as shown in Figure 3b, the $\mathbb{Z}_2$ topological invariant takes the nontrivial value [34]. The above Hamiltonian is regularized on the square lattice as

$$\mathcal{H}_0(k_x, k_y) \rightarrow \frac{2 - \cos k_x - \cos k_y}{m} \sigma_0 s_0 - \epsilon \sigma_x s_0 + \alpha(s_y \sin k_x - s_x \sin k_y) \sigma_z. \tag{40}$$

We consider the six types of odd-parity pair potentials, which are summarized in Table 2.
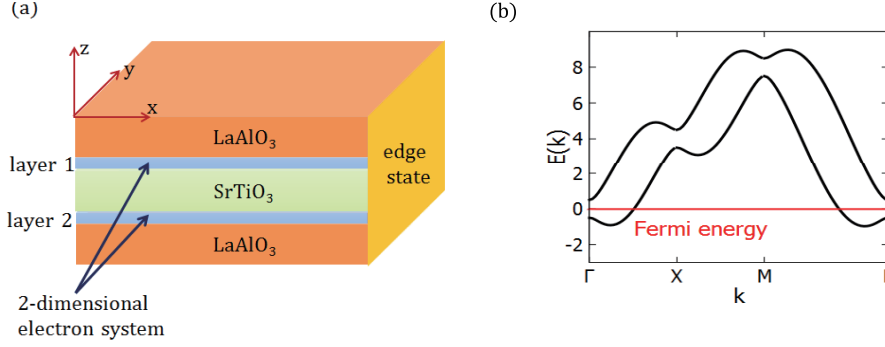
Figure 3. Schematic view of the Rashba bilayer between LaAlO$_3$ and SrTiO$_3$ [34]. (**a**) Two-dimensional electron gases are formed in the interfaces. The energy dispersions of the finite system with the edge normal to the x axis are shown in Figure 5 for possible pair potentials; (**b**) The energy dispersion of the Hamiltonian Equation (38) in the normal state. The Fermi energy is located at $E = 0$. The parameters are taken as $m = 0.5$, $\varepsilon = 0.5$, $\alpha = 2$.

Table 2. Irreducible representations Γ of odd-parity pair potentials Δ in the bilayer Rashba superconductor under the D_{4h} symmetry. $W[U, x]$ is the winding number related to Majorana fermions on the (100) edge and S denotes the direction of its Ising spin. These are taken from Table A1. **0** denotes the absence of Majorana fermion.

Γ	$W[U, x]$	Δ	S
A_{1u}	$W[C_2'(x)]$	$\sigma_y s_z$	x
A_{2u}	$W[\sigma_v(xz), x]$	$\sigma_z s_0$	y
B_{1u}	$W[C_2'(x)]$	$\sin k_x \sin k_y \sigma_z s_0$	x
B_{2u}	$W[\sigma_v(xz), x]$	$(\cos k_x - \cos k_y)\sigma_z s_0$	y
$E_u(x)$	0	$\sigma_y s_y$	0
$E_u(y)$	$W[\sigma_h, x]$	$\sigma_y s_x$	z

We show that the winding numbers $W[U, x_\perp]$ which associated with the Majorana fermions on the (100) surface for each pairing. From Table 2, the A_{1u} [$\Delta(k_x, k_y) = \Delta\sigma_y s_z$], A_{2u} [$\Delta(k_x, k_y) = \Delta\sigma_z s_0$], B_{2u} [$\Delta(k_x, k_y) = \Delta(\cos k_x - \cos k_y)\sigma_z s_0$], and $E_u(y)$ [$\Delta(k_x, k_y) = \Delta\sigma_y s_x$] pairing may have nonzero winding numbers $W[C_2'(x)]$, $W[\sigma_v, x_{\sigma_v} \neq z]$, $W[\sigma_v, x_{\sigma_v} \neq z]$, and $W[\sigma_h, x]$, respectively. The B_{1u} pairing, $\Delta(k_x, k_y) = \Delta \sin k_x \sin k_y \sigma_z s_0$, on the other hand, does not open the gap at the time-reversal-invariant momenta, $k_y = 0, \pi$, so that the winding number is ill-defined. The $E_u(x)$ pairing has no Majorana fermion on the (100) surface. The symmetry operations and the corresponding chiral operators are represented by

$$C_2'(x) = \sigma_x(-is_x), \ \sigma_v(xz) = \sigma_0(-is_y), \ \sigma_h = \sigma_x(-is_z), \tag{41}$$

and

$$\Gamma_{C_2'(x)} = iC_2'(x)\tau_y, \ \Gamma_{\sigma_v(xz)} = i\sigma_v(xz)\tau_y, \ \Gamma_{\sigma_h} = i\sigma_h\tau_y. \tag{42}$$

The winding number is calculated to be

$$W[U, \boldsymbol{x}] = \int_{-\pi}^{\pi} \frac{dk_x}{2\pi} \frac{\partial}{\partial k_x} \arg \det q(k_y),$$ (43)

where $q(k_y)$ is the off-diagonal part of the Hamiltonian in the chiral basis (see Equation (A13)).

Figure 4 shows the winding of $\arg \det q(k_y)$ for each pairing, which immediately tells us that the winding number is obtained to be $W[C_2'(x)] = -2$, $W[\sigma_v(xz), \boldsymbol{x}] = -2$, $W[\sigma_v(xz), \boldsymbol{x}] = 2$, $W[\sigma_h, \boldsymbol{x}] = 2$, for A_{1u}, A_{2u}, B_{2u}, and $E_u(y)$ pairings, respectively. $|W(U, \boldsymbol{x})| = 2$ means that a Majorana Kramers pair appears on the (100) edge. As a result, the systems are, indeed, topological superconductors with finite winding numbers predicted by our general theory.
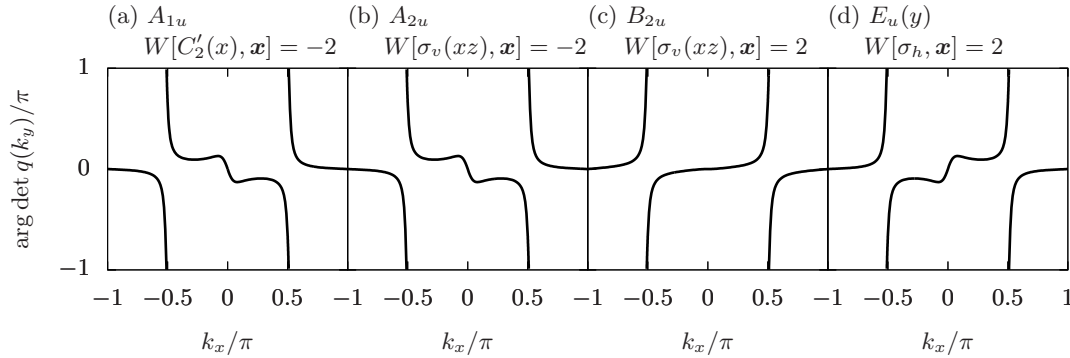
Figure 4. Winding of the phase (integrand of $W[U, \boldsymbol{x}]$) for the (**a**) A_{1u}; (**b**) A_{2u}; (**c**) B_{2u}; and (**d**) $E_u(y)$ pairings. The winding numbers are obtained to be $W[C_2'(x)] = -2$, $W[\sigma_v(xz), \boldsymbol{x}] = -2$, $W[\sigma_v(xz), \boldsymbol{x}] = 2$, and $W[\sigma_h, \boldsymbol{x}] = 2$, for cases (**a**–**d**), respectively.

Next, we verify the above result and the predicted Majorana Ising spins, which are shown in Table 2, from the energy spectra of finite-sized systems. The corresponding finite-sized Hamiltonian defined in ($1 \leq x \leq N_x$) along the x direction has the form $H(k_y) = H_0(k_y) + \tilde{\Delta}(k_y)$ with

$$\begin{aligned}
H_0(k_y) = \sum_{n=1}^{N_x} c_n^\dagger(k_y) &\left[\left(\frac{2 - \cos k_y}{m} + \mu \right) \sigma_0 s_0 + \alpha \sin k_y \sigma_z s_x + \varepsilon \sigma_x s_0 \right] \tau_z c_n(k_y) \\
&+ \left[\sum_{n=1}^{N_z - 1} c_n^\dagger(k_y) \left(\frac{1}{2m} \sigma_0 s_0 + \frac{\alpha}{2} \sigma_z s_y \right) \tau_z \tilde{c}_{n+1}(k_y) + \text{h.c.} \right],
\end{aligned}$$ (44)

where $c_n(k_y) = (c_{n\uparrow}(k_y), c_{n\downarrow}(k_y), c_{n\downarrow}^\dagger(-k_y), -c_{n\uparrow}^\dagger(-k_y))^{\mathrm{T}}$ is the annihilation operator of electron with momentum k_y on the n-th site. The pair-potential term is given by

$$\tilde{\Delta}(k_y) = \begin{cases}
\displaystyle\sum_{n=1}^{N_x} c_n^\dagger(k_y) \Delta \sigma_y s_z \tau_x c_n(k_y), & \text{for } A_{1u}, \\[2ex]
\displaystyle\sum_{n=1}^{N_x} c_n^\dagger(k_y) \Delta \sigma_z s_0 \tau_x c_n(k_y), & \text{for } A_{2u}, \\[2ex]
\displaystyle\sum_{n=1}^{N_x - 1} c_{n+1}^\dagger(k_y) i\Delta \sin k_y \sigma_z s_0 \tau_x c_n(k_y) + \text{h.c.}, & \text{for } B_{1u}, \\[2ex]
\displaystyle\sum_{n=1}^{N_x} c_n^\dagger(k_y) \Delta \cos k_y \sigma_z s_0 \tau_x c_n(k_y) - \frac{1}{2} \left(\sum_{n=1}^{N_x - 1} c_{n+1}^\dagger(k_y) \Delta \sigma_z s_0 \tau_x c_n(k_y) + \text{h.c.} \right), & \text{for } B_{2u}, \\[2ex]
\displaystyle\sum_{n=1}^{N_x} c_n^\dagger(k_y) \Delta \sigma_y s_y \tau_x c_n(k_y), & \text{for } E_u(x), \\[2ex]
\displaystyle\sum_{n=1}^{N_x} c_n^\dagger(k_y) \Delta \sigma_y s_x \tau_x c_n(k_y), & \text{for } E_u(y).
\end{cases}$$ (45)

We calculate the energy spectrum in the presence of a Zeeman field along *x*, *y*, and *z* directions, which are expressed by the Hamiltonian

$$H_{\mathbf{B}} = \sum_{n=1}^{N_x} c_n^{\dagger}(k_y) \left(\mathbf{B} \cdot \frac{g\mu_{\mathrm{B}}}{2}\mathbf{s} \right) c_n(k_y) = \sum_{n=1}^{N_x} c_n^{\dagger}(k_y)\mathbf{h} \cdot \mathbf{s}c_n(k_y). \tag{46}$$

For topological superconducting states, the Majorana zero modes still remain gapless in the presence of a magnetic field perpendicular to the Majorana Ising spin. The direction of the Majorana Ising spin for each pair potential is derived by the general theory studied in the previous section and shown in Table 2. This is verified by the numerical results, which are shown in Figure 5.
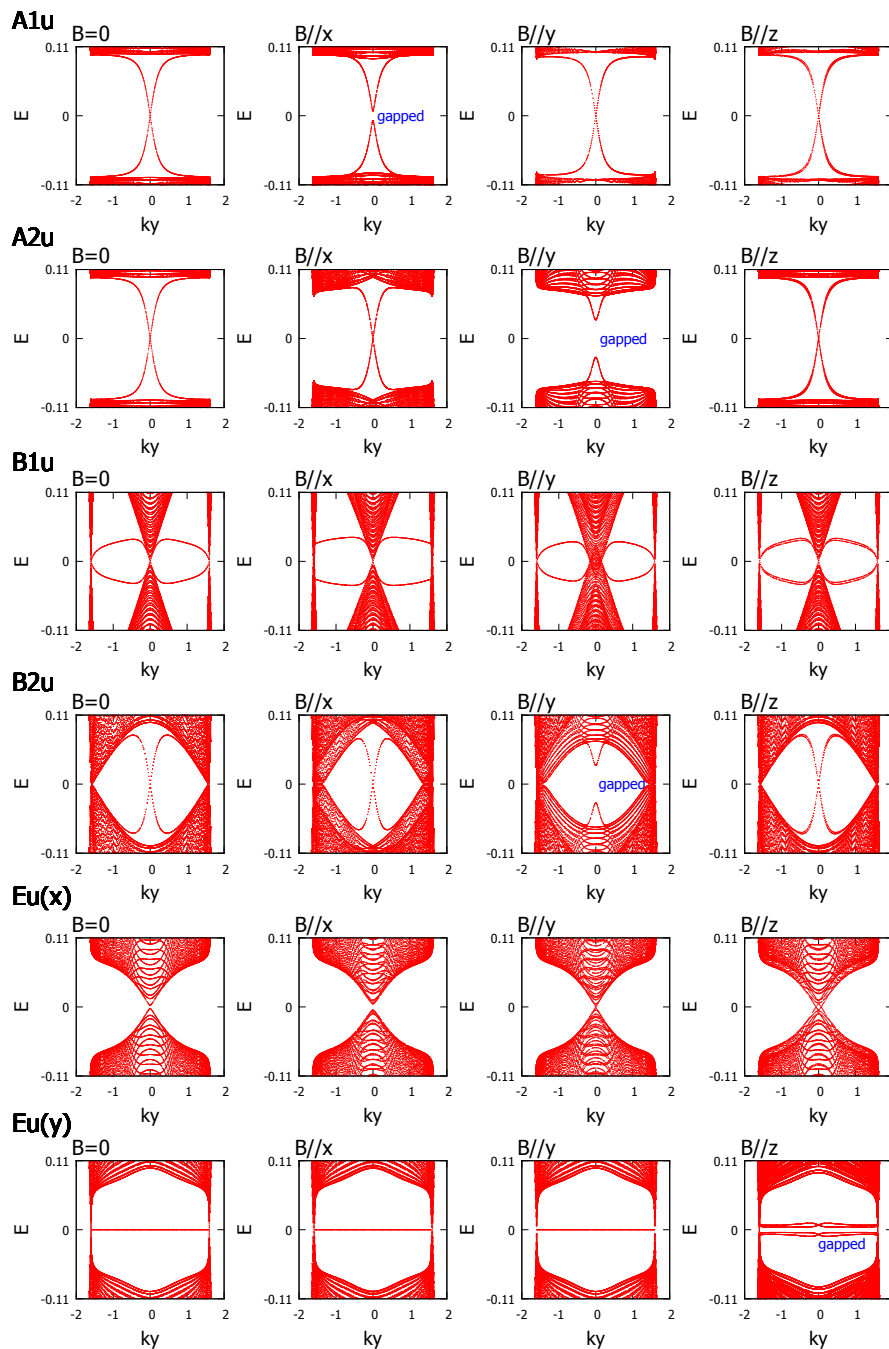
Figure 5. Energy spectra for odd parity pair potentials for $\Delta = 0.1$ and $h = 0.03$. The parameters are the same as in Figure 3b.

For the A_{1u} pairing, Majorana zero modes exist at $k_y = 0$ for the cases of $\boldsymbol{B} \parallel \boldsymbol{y}$ and of $\boldsymbol{B} \parallel \boldsymbol{z}$, while they vanish and a gap is generated for the case of $\boldsymbol{B} \parallel \boldsymbol{x}$. For the A_{2u} pairing, Majorana zero modes vanish only for the case of $\boldsymbol{B} \parallel \boldsymbol{y}$. Note that the A_{2u}-pairing state under a magnetic field along the z direction is the same as the pair-density-wave (PDW) state studied in Ref. [35,36]. There is no Majorana zero mode for the B_{1u} pairing because the bulk superconducting gap closes at $k_y = 0$. For the B_{2u} pairing, on the other hand, the bulk superconducting gap closes at $k_y \neq 0$ and remains finite at $k_y = 0$. Hence Majorana zero modes are emerged at $k_y = 0$ and killed by a magnetic field along the y direction. The E_u pairings are similar to the B_{1u} and B_{2u} pairings. The bulk gap vanishes at $k_y = 0$ for the $E_u(x)$ pairing but survives for the $E_u(y)$ paring. The emerged Majorana zero modes are gapped only when a magnetic field is applied along the z direction. Namely, A_{1u}, A_{2u}, B_{2u}, and $E_u(y)$ pair potentials, Majorana zero modes vanish for a specific direction of magnetic field, i.e., the Majorana zero modes respond to the field as a Ising spin. This results on the Majorana Ising spins totally coincide with those in Table 2.

6. Conclusions

We have derived possible nonzero topological invariants and the direction of Majorana Ising spin for each irreducible representation of pair potential for time-reversal-invariant superconductors. The obtained result is the detailed classification in the class-DIII superconductors in one spatial dimension. Another point of view is a topological extension to the classification of superconducting pair potential. Our result is general and does not depend on the detail of systems therefore it is useful for all researchers on superconducting materials. The anisotropy can be detected by the tunneling spectroscopy under a magnetic field or with a ferromagnetic junction because a zero-bias peak appears in the presence of the Majorana zero modes [37].

Several examples have been shown for the bilayer Rashba superconductor, D_{4h}, C_{4v}, C_{2v} point groups, and the *Pmma* space group. In the other point groups, D_{6h}, D_{3d}, and D_{3h}, another type of anisotropic response can arise. This will be demonstrated in a separate paper. As for the topological invariants, we focused only on the $\mathbb{Z}$ topological invariant in the paper. To complete the classification, we also need to clarify the $\mathbb{Z}_2$ topological invariant and the related Majorana Ising spins. This issue will be also addressed in a future paper.

Author Contributions: Y.X. carried out numerical calculations. Y.X., S.K., and A.Y. obtained the necessary conditions for the nonzero topological invariants. A.Y., M.S. and Y.T. discussed the results and wrote the paper.

Conflicts of Interest: The authors declare no conflict of interest.

Abbreviations

The following abbreviations are used in this manuscript:

BdG   Bogoliubov-de Gennes

Appendix A. Bulk-Edge Correspondence in a Lattice Model

In this Appendix, we derive the bulk-edge correspondence, i.e., the number of zero-energy end states equals to the one-dimensional winding number W, in lattice models.

Appendix A.1. Number of Edge States

Firstly, we derive the number of zero-energy edge states in the corresponding lattice model with the *r*-th neighbor hoppings, generalizing the discussion by W. Izumida et al. [33]. The Hamiltonian is expressed in a semi-infinite lattice defined in $n \leq 0$ as

$$H = \sum_{n \leq 0} c_n^\dagger \epsilon c_n + \sum_{q=1}^r \sum_{n \leq -q} \left(c_n^\dagger t_q c_{n+q} + c_{n+q}^\dagger t_q^\dagger c_n \right), \ \epsilon = \epsilon_1 \tau_1 + \epsilon_3 \tau_3, \ t_q = t_{q1} \tau_1 + t_{q3} \tau_3. \tag{A1}$$

The Schrödinger equation is given by

$$E \psi_n = \epsilon \psi_n + \sum_{q=1}^r \left(t_q \psi_{n+1} + t_q^\dagger \psi_{n-1} \right), \tag{A2}$$

where ψ_n is the wavefuntion at the *n*-th site. Now we derive zero-energy ($E = 0$) end states, whose fundamental solution of wavefunction has the form

$$\psi_n = \lambda^{-n} \phi, \tag{A3}$$

for $|\lambda| < 1$ in the left-half space $n \leq 0$. Substituting the above form into the Schrödinger equation, one obtains

$$\left[\epsilon + \sum_{q=1}^r \left(t_q \lambda^{-q} + t_q^\dagger \lambda^q \right) \right] \phi = 0. \tag{A4}$$

Multiplying τ_3 to the above equation, one finds that the zero-energy states are chirality eigenstates, i.e., ϕ is given by $\phi = \phi_\tau \chi_\tau$ for $\tau_2 \chi_\tau = \tau \chi_\tau$ with $\tau = \pm 1$ chirality. ϕ_τ is obtain by solving $q_\tau(\lambda) \phi_\tau = 0$ with

$$q_\tau(\lambda) = \epsilon_1 i\tau + \epsilon_3 + \sum_{q=1}^r \left\{ [t_{q1} i\tau + t_{q3}] \lambda^{-q} + [t_{q1}^\dagger i\tau + t_{q3}^\dagger] \lambda^q \right\}, \tag{A5}$$

For a nontrivial solution of ϕ_τ, the secular equation $\det q_\tau(\lambda) = 0$ holds and has $[r \dim H(k)]$ solutions. As a result, the fundamental solutions for the zero-energy end states are obtained to be

$$\psi_{\tau,n} = \lambda_j^{-n} \phi_\tau(\lambda_j) \chi_\tau, \ \lambda_j \in Q_\tau = \{\lambda | \det q_\tau(\lambda) = 0, |\lambda| < 1\}, \ q_\tau(\lambda_j) \phi_\tau(\lambda_j) = 0. \tag{A6}$$

The number of the independent solutions for the definite chirality τ is $|Q_\tau|$.

So as to obtain the physical solutions with a definite chirality τ, a boundary condition is imposed on the system end $n = 0$, e.g., the fixed boundary condition $\psi_{\tau,q} = 0$ for $q \geq -r + 1$. The boundary condition gives $[r \dim H(k)/2]$ conditions. Consequently, one obtains the number of the zero-energy end states with the chirality of τ to be

$$N_\tau = \left| |Q_\tau| - \frac{r \dim H(k)}{2} \right| \theta \left(|Q_\tau| - \frac{r \dim H(k)}{2} \right). \tag{A7}$$

One obtains only the trivial solution, $\psi_{\tau,n} = 0$, for $|Q_\tau| = r \dim H(k)/2$. $\det q_\tau(\lambda) = 0$ is equivalent to $\det q_\tau(\lambda)^* = 0$, which is explicitly shown as

$$\det \left\{ \epsilon_1(-i\tau) + \epsilon_3 + \sum_{q=1}^r [t_{q1}(-i\tau) + t_{q3}] \lambda^{q*} + \sum_{q=1}^r [t_{q1}^\dagger(-i\tau) + t_{q3}^\dagger] \lambda^{-q*} \right\} = 0. \tag{A8}$$

This means that if solution is given by λ for $\tau = +1$ then the solution for $\tau = -1$ is given by λ^{*-1}. Namely, one finds

$$|Q_+| + |Q_-| = r \dim H(k). \tag{A9}$$

From the above condition, the possible (N_+, N_-) are classified into three cases:

$$(N_+, N_-) = \begin{cases} (N, 0), & |Q_+| > \dfrac{r \dim H(k)}{2}, \\ (0, 0), & |Q_+| = \dfrac{r \dim H(k)}{2}, \\ (0, N), & |Q_+| < \dfrac{r \dim H(k)}{2}. \end{cases} \tag{A10}$$

Appendix A.2. Bulk-Edge Correspondence

Next, we calculate the winding number of the translational-invariant system, which is described by

$$H(k) = \epsilon + \sum_{q=1}^{r} \left(t_q e^{ikq} + t_q^\dagger e^{-ikq} \right). \tag{A11}$$

The winding number is given by

$$\begin{aligned} W &= \frac{i}{4\pi} \int_{-\pi}^{\pi} dk \, \mathrm{tr}\left[\Gamma H(k)^{-1} \frac{\partial H(k)}{\partial k} \right] \\ &= \frac{i}{4\pi} \int_{-\pi}^{\pi} dk \, \mathrm{tr}\left[\begin{pmatrix} 1 & 0 \\ 0 & -1 \end{pmatrix} \begin{pmatrix} 0 & q^{\dagger-1}(k) \\ q^{-1}(k) & 0 \end{pmatrix} \begin{pmatrix} 0 & \dfrac{\partial q(k)}{\partial k} \\ \dfrac{\partial q(k)^\dagger}{\partial k} & 0 \end{pmatrix} \right] \\ &= \mathrm{Im} \int_{-\pi}^{\pi} \frac{dk}{2\pi} \frac{\partial}{\partial k} \ln \det q(k). \end{aligned} \tag{A12}$$

In this way, the basis in which the chiral operator is diagonalized makes it easy to calculate the winding number. Then we first off-diagonalize the Hamiltonian as

$$\tilde{H}(k) = \Lambda_3(k)\tau_1 + \Lambda_1(k)\tau_2, \quad \Lambda_j(k) = \epsilon_j + \sum_{q=1}^{r} \left(t_{qj} e^{ikq} + t_{qj}^\dagger e^{-ikq} \right). \tag{A13}$$

This reduces the winding number to be

$$\begin{aligned} W &= \mathrm{Im} \int_{-\pi}^{\pi} \frac{dk}{2\pi} \frac{\partial}{\partial k} \ln \det\left[\Lambda_3(k) - i\Lambda_1(k) \right] = \mathrm{Im} \int_{-\pi}^{\pi} \frac{dk}{2\pi} \frac{\partial}{\partial k} \ln \det q_-(e^{-ik}) \\ &= -\mathrm{Im} \oint_{|\lambda|=1} \frac{d\lambda}{2\pi} \frac{\partial}{\partial \lambda} \ln \det q_-(\lambda) = -|Q_-| + \frac{r}{2} \dim H(k), \end{aligned} \tag{A14}$$

where the integral runs over the unit circle in the complex λ plane along the counter-clockwise direction. The last line of the above equation is derived with the use of the argument principle because $\det q_\tau(\lambda)$ has $|Q_\tau|$ zeros within the unit circle and is asymptotically given by

$$\det q_\tau(\lambda) \sim \frac{1}{\lambda^{r[\dim H(k)]/2}} \det(t_{r1} i\tau + t_{r3}), \tag{A15}$$

which has the order-$[r \dim H(k)]/2$ pole. Thus $W = -N_-$ for $|Q_-| > [r \dim H(k)]/2$. Because W is an integer, the above relation is rewritten as

$$W = W^* = -\mathrm{Im} \int_{-\pi}^{\pi} \frac{dk}{2\pi} \frac{\partial}{\partial k} \ln \det\left[\Lambda_3(k) + i\Lambda_1(k) \right] = |Q_+| - \frac{r}{2} \dim H(k). \tag{A16}$$

The winding number equals $W = N_+$ for $|Q_+| > [r \dim H(k)]/2$. We finally arrive at the bulk-edge correspondence:

$$W = N_+ - N_-. \tag{A17}$$

Appendix B. Representation of Symmetry Operation

Order-2 symmetry operations of space groups are decomposed into the real-space part $O(\boldsymbol{\tau})$ and spin part Σ;

$$\{U|\boldsymbol{\tau}\} = O(\boldsymbol{\tau})\Sigma, \tag{A18}$$

where $\boldsymbol{\tau}$ is half a primitive translation vector. The spin part is independent of the translation. For (screw) rotations, Σ is taken to be along the (screw) rotational axis. For (glide) reflections, on the other hand, Σ is perpendicular to the (glide) reflection plane, $\Sigma = \boldsymbol{s} \cdot \boldsymbol{n}$, where s_x, s_y, s_z are the Pauli matrices and $\boldsymbol{n}$ is the unit vector normal to the plane. Note that $\Sigma^2 = 1$ and Σ anticommutes with time reversal, $\{\Sigma, \mathcal{T}\} = 0$. The real-space part $O(\boldsymbol{\tau})$ commutes with time reversal $[O(\boldsymbol{\tau}), \mathcal{T}] = 0$ and satisfies the following relation

$$O(\boldsymbol{\tau})^2 = \{1|2\boldsymbol{\tau}\} = e^{i2\boldsymbol{k}\cdot\boldsymbol{\tau}}, \tag{A19}$$

in the momentum space. Therefore, the chiral operator is given by

$$\Gamma_{\{U|\boldsymbol{\tau}\}} = e^{-i\boldsymbol{k}\cdot\boldsymbol{\tau}}\{U|\boldsymbol{\tau}\}\tau_y, \ \Gamma^2_{\{U|\boldsymbol{\tau}\}} = 1. \tag{A20}$$

In this choice, we obtain the commutation relation of $\Gamma_{\{U|\boldsymbol{\tau}\}}$ and time reversal $\mathcal{T}$;

$$\{\mathcal{T}, \Gamma_{\{U|\boldsymbol{0}\}}\} = 0, \tag{A21}$$

$$\{\mathcal{T}, \Gamma_{\{U|\boldsymbol{\tau}\}}\} = 0, \ \text{for } e^{i\boldsymbol{k}\cdot\boldsymbol{\tau}} = 1, \tag{A22}$$

$$[\mathcal{T}, \Gamma_{\{U|\boldsymbol{\tau}\}}] = 0, \ \text{for } e^{i\boldsymbol{k}\cdot\boldsymbol{\tau}} = \pm i. \tag{A23}$$

For nonsymmorphic symmetry operations, $\boldsymbol{\tau} \neq \boldsymbol{0}$, representations at the zone center are different from those at the zone boundary.

Appendix C. Tables for Irreducible Representations and Majorana Ising Spins

We show several examples of topological invariants $W[\tilde{U}_i, \boldsymbol{x}_\perp]$ under the D_{4h}, C_{4v}, and C_{2v} point-group symmetries in Table A1. The nonzero topological invariants, $W[\tilde{U}_i, \boldsymbol{x}_\perp]$, are derived by applying Equation (23) to each representation. We also show the case for the space group *Pmma* that is

$$\{\{C_2(z)|\boldsymbol{a}/2\}, \{C_2(x)|\boldsymbol{a}/2\}, \{C_2(y)|\boldsymbol{0}\}, \{\sigma(xy)|\boldsymbol{a}/2\}, \{\sigma(yz)|\boldsymbol{a}/2\}, \{\sigma(xz)|\boldsymbol{0}\}\}, \tag{A24}$$

in Table A2, solving Equation (20) and the commutators, $p(\tilde{U}_j, \tilde{U}_l)$, which are defined by $U_j U_l = p(U_j, U_l) U_l U_j$, for the symmetry operations U_j in the *Pmma* group (Table A3). $p(U_j, U_l)$ is calculated in the same manner as in Ref. [38]. Note that the topological invariants for glide reflections vanish, $W[\{U|\boldsymbol{a}/2\}, \boldsymbol{x}_\perp] = 0$, for $k_x a_x = \pi$, as discussed in Section 3.3. And also, Majorana fermions do not appear on the (yz) plane even for $W[\{U|\boldsymbol{a}/2\}, \boldsymbol{x}] \neq 0$ since the nonsymmorphic symmetry involving the half translation of $\boldsymbol{a}/2$ is broken on the (yz) surface. Finally, the Majorana Ising spin protected by $W[\tilde{U}_i, \boldsymbol{x}_\perp]$ is obtained to be parallel to the rotational axis for $\tilde{U}_i = \tilde{C}_2$ or normal to the mirror plane for $\tilde{U}_i = \sigma$, respectively, as explained in Section 2.

Table A1. Possible topological invariants $W[\tilde{U}_i, x_\perp]$ and the direction of the Majorana Ising spin on the given surfaces for each irreducible representation of D_{4h}, C_{4v}, and C_{2v}. The surface is denoted by the mirror index (hkl) or the Cartesian coordinate $(x_i x_j)$. x_σ of $W[\sigma, x_\sigma]$ is the direction normal to the surface and is on the σ mirror plane. The C_2' axis is set to the x axis. The representations $E_u(x)$ and $E_u(y)$ are defined in the bottom table.

D_{4h}	$W[U, x_\perp]$	(001)	(100)	(110)	
A_{1u}	$W[C_n], W[C_2'], W[C_2'']$	[001]	[100]	[110]	
A_{2u}	$W[\sigma_v, x_{\sigma_v} \neq [001]], W[\sigma_d, x_{\sigma_d} \neq [001]]$	0	[010]	[1$\bar{1}$0]	
B_{1u}	$W[C_2'], W[\sigma_d, x_{\sigma_d} \neq [001]]$	0	[100]	[1$\bar{1}$0]	
B_{2u}	$W[C_2''], W[\sigma_v, x_{\sigma_v} \neq [001]]$	0	[010]	[110]	

D_{4h}	$W[U, x_\perp]$	(001)	(100)	(010)	(110)
$E_u(x)$	$W[\sigma_v(010), x_{\sigma_v(010)} \neq [100]], W[\sigma_h, x_{\sigma_h} \neq [100]]$	[010]	0	[001]	[001]
$E_u(y)$	$W[\sigma_v(100), x_{\sigma_v(100)} \neq [010]], W[\sigma_h, x_{\sigma_h} \neq [010]]$	[100]	[001]	0	[001]

C_{4v}	$W[U, x_\perp]$	(001)	(100)	(110)		
A_1	$W[\sigma_v, x_{\sigma_v} \neq z], W[\sigma_d, x_{\sigma_d} \neq z]$	0	[010]	[1$\bar{1}$0]		
A_2	$W[C_2]$	[001]	0	0		
B_1	$W[\sigma_v, x_{\sigma_v} \neq z]$	0	[010]	0		
B_2	$W[\sigma_d, x_{\sigma_d} \neq z]$	0	0	[1$\bar{1}$0]		
$E(x)$	$W[\sigma_v(zx), x_{\sigma_v(zx)} \neq x]$			[010]	0	0
$E(y)$	$W[\sigma_v(yz), x_{\sigma_v(yz)} \neq y]$			[100]	0	0

C_{2v}	$W[U, x_\perp]$	(xy)	(yz)	(zx)
A_1	$W[\sigma_v(zx), x_{\sigma_v(zx)} \neq z], W[\sigma_v(yz), x_{\sigma_v(yz)} \neq z]$	0	y	x
A_2	$W[C_2]$	z	0	0
B_1	$W[\sigma_v(zx), x_{\sigma_v(zx)} \neq x]$	y	0	0
B_2	$W[\sigma_v(yz), x_{\sigma_v(yz)} \neq y]$	x	0	0

D_{4h}	C_2	$C_2'(x)$	$C_2'(y)$	σ_h	$\sigma_v(yz)$	$\sigma_v(xz)$
$E_u(x)$	−	+	−	+	−	+
$E_u(y)$	−	−	+	+	+	−

Table A2. Possible topological invariants $W[\tilde{U}_i, x_\perp]$ in the *Pmma* space group for $k_x a_x = 0$ (upper) and $k_x a_x = \pi$ (lower).

Pmma	$W[U, x_\perp](k_x = 0)$	(xy)	(yz)	(xz)
A_g	0	0	0	0
B_{1g}	0	0	0	0
B_{2g}	0	0	0	0
B_{3g}	0	0	0	0
A_u	$W[\{C_2(z)|a/2\}], W[\{C_2(x)|a/2\}], W[\{C_2(y)|0\}]$ $W[\{\sigma(xy)|a/2\}, x_{\sigma(xy)} \neq x, y]$ $W[\{\sigma(yz)|a/2\}, x_{\sigma(yz)} \neq y, z]$ $W[\{\sigma(xz)|0\}, x_{\sigma(xz)} \neq x, z]$	z	0	x
B_{1u}	$W[\{\sigma(xy)|a/2\}, x_{\sigma(xy)} \neq x, y]$ $W[\{\sigma(yz)|a/2\}, x_{\sigma(yz)} \neq z]$ $W[\{\sigma(xz)|0\}, x_{\sigma(xz)} \neq z]$	0	y	x
B_{2u}	$W[\{\sigma(xy)|a/2\}, x_{\sigma(xy)} \neq y]$ $W[\{\sigma(yz)|a/2\}, x_{\sigma(yz)} \neq y\}]$ $W[\{\sigma(xz)|0\}, x_{\sigma(xz)} \neq x, z]$	x	0	0
B_{3u}	$W[\{\sigma(xy)|a/2\}, x_{\sigma(xy)} \neq x]$ $W[\{\sigma(yz)|a/2\}, x_{\sigma(yz)} \neq y, z]$ $W[\{\sigma(xz)|0\}, x_{\sigma(xz)} \neq x]$	y	0	z

Table A2. *Cont.*

Pmma	$W[U, x_\perp](k_x a_x = \pi)$	(xy)	(yz)	(xz)
A_g	$W[\{\sigma(yz)|a/2\}, x_{\sigma(yz)} \neq z]$	**0**	**0**	x
B_{1g}	$W[\{C_2(z)|a/2\}]$	z	**0**	**0**
B_{2g}	$W[\{\sigma(xy)|a/2\}, x_{\sigma(xy)} \neq y]$ $W[\{\sigma(yz)|a/2\}, x_{\sigma(yz)} \neq y,z]$ $W[\{\sigma(xy)|a/2\}, x_{\sigma(xy)} \neq x,y]$ $W[\{\sigma(yz)|a/2\}, x_{\sigma(yz)} \neq y,z]$	**0**	**0**	**0**
B_{3g}	$W[\{\sigma(xy)|a/2\}, x_{\sigma(xy)} \neq x,y]$ $W[\{\sigma(yz)|a/2\}, x_{\sigma(yz)} \neq y]$	x	**0**	**0**
A_u	$W[\{\sigma(xz)|0\}, x_{\sigma(xz)} \neq x,z]$	**0**	**0**	**0**
B_{1u}	$W[\{\sigma(xz)|0\}, x_{\sigma(xz)} \neq z]$	**0**	y	**0**
B_{2u}	$W[\{C_2(y)|0\}], W[\{\sigma(xz)|0\}, x_{\sigma(xz)} \neq x,z]$	**0**	**0**	y
B_{3u}	$W[\{C_2(x)|a/2\}], W[\{\sigma(xz)|0\}, x_{\sigma(xz)} \neq x]$	y	**0**	**0**

Table A3. Commutator $p(U_j, U_l) = U_j^{-1} U_l^{-1} U_j U_l$ for the *Pmma* group. A row and column correspond to U_j and U_l, respectively.

	$\{C_2(z)|a/2\}$	$\{C_2(x)|a/2\}$	$\{C_2(y)|0\}$	$\{\sigma(xy)|a/2\}$	$\{\sigma(yz)|a/2\}$	$\{\sigma(xz)|0\}$
$\{C_2(z)|a/2\}$	1	$-e^{ik_x a_x}$	$-e^{ik_x a_x}$	$e^{ik_x a_x}$	-1	-1
$\{C_2(x)|a/2\}$	$-e^{-ik_x a_x}$	1	$-e^{-ik_x a_x}$	-1	$e^{ik_x a_x}$	-1
$\{C_2(y)|0\}$	$-e^{-ik_x a_x}$	$-e^{ik_x a_x}$	1	$-e^{ik_x a_x}$	$-e^{ik_x a_x}$	1
$\{\sigma(xy)|a/2\}$	$e^{-ik_x a_x}$	-1	$-e^{-ik_x a_x}$	1	$-e^{-ik_x a_x}$	-1
$\{\sigma(yz)|a/2\}$	-1	$e^{ik_x a_x}$	$-e^{-ik_x a_x}$	$-e^{ik_x a_x}$	1	-1
$\{\sigma(xz)|0\}$	-1	-1	1	-1	-1	1

References

1. Hasan, M.Z.; Kane, C.L. *Colloquium*: Topological insulators. *Rev. Mod. Phys.* **2010**, *82*, 3045–3067.
2. Qi, X.L.; Zhang, S.C. Topological insulators and superconductors. *Rev. Mod. Phys.* **2011**, *83*, 1057–1110.
3. Tanaka, Y.; Sato, M.; Nagaosa, N. Symmetry and Topology in Superconductors—Odd-Frequency Pairing and Edge States. *J. Phys. Soc. Jpn.* **2012**, *81*, 011013.
4. Ando, Y. Topological Insulator Materials. *J. Phys. Soc. Jpn.* **2013**, *82*, 102001.
5. Buchholtz, L.J.; Zwicknagl, G. Identification of p-wave superconductors. *Phys. Rev. B* **1981**, *23*, 5788–5796.
6. Hara, J.; Nagai, K. A Polar State in a Slab as a Soluble Model of p-Wave Fermi Superfluid in Finite Geometry. *Prog. Theor. Phys.* **1986**, *76*, 1237–1249.
7. Hu, C.R. Midgap surface states as a novel signature for d_{xa}^2-x_b^2-wave superconductivity. *Phys. Rev. Lett.* **1994**, *72*, 1526–1529.
8. Tanaka, Y.; Kashiwaya, S. Theory of Tunneling Spectroscopy of d-Wave Superconductors. *Phys. Rev. Lett.* **1995**, *74*, 3451–3454.
9. Nayak, C.; Simon, S.H.; Stern, A.; Freedman, M.; Das Sarma, S. Non-Abelian anyons and topological quantum computation. *Rev. Mod. Phys.* **2008**, *80*, 1083–1159.
10. Schnyder, A.P.; Ryu, S.; Furusaki, A.; Ludwig, A.W.W. Classification of topological insulators and superconductors in three spatial dimensions. *Phys. Rev. B* **2008**, *78*, 195125.
11. Kitaev, A. Periodic table for topological insulators and superconductors. *AIP Conf. Proc.* **2009**, *1134*, 22–30.
12. Ryu, S.; Schnyder, A.P.; Furusaki, A.; Ludwig, A.W.W. Topological insulators and superconductors: Tenfold way and dimensional hierarchy. *New J. Phys.* **2010**, *12*, 065010.
13. Sato, M.; Fujimoto, S. Topological phases of noncentrosymmetric superconductors: Edge states, Majorana fermions, and non-Abelian statistics. *Phys. Rev. B* **2009**, *79*, 094504.
14. Chung, S.B.; Zhang, S.C. Detecting the Majorana Fermion Surface State of ^{3}He-*B* through Spin Relaxation. *Phys. Rev. Lett.* **2009**, *103*, 235301.

15. Nagato, Y.; Higashitani, S.; Nagai, K. Strong Anisotropy in Spin Susceptibility of Superfluid 3He-B Film Caused by Surface Bound States. *J. Phys. Soc. Jpn.* **2009**, *78*, 123603.

16. Volovik, G. Topological superfluid 3He-B in magnetic field and ising variable. *JETP Lett.* **2010**, *91*, 201–205.

17. Shindou, R.; Furusaki, A.; Nagaosa, N. Quantum impurity spin in Majorana edge fermions. *Phys. Rev. B* **2010**, *82*, 180505.

18. Silaev, M.A. Majorana states and longitudinal NMR absorption in a ^{3}He-*B* film. *Phys. Rev. B* **2011**, *84*, 144508.

19. Yada, K.; Sato, M.; Tanaka, Y.; Yokoyama, T. Surface density of states and topological edge states in noncentrosymmetric superconductors. *Phys. Rev. B* **2011**, *83*, 064505.

20. Mizushima, T.; Machida, K. Effects of Majorana Edge Fermions on Dynamical Spin Susceptibility in Topological Superfluid 3He-B. *J. Low Temp. Phys.* **2011**, *162*, 204–211.

21. Mizushima, T.; Sato, M.; Machida, K. Symmetry Protected Topological Order and Spin Susceptibility in Superfluid ^{3}He-*B*. *Phys. Rev. Lett.* **2012**, *109*, 165301.

22. Mizushima, T.; Sato, M. Topological phases of quasi-one-dimensional fermionic atoms with a synthetic gauge field. *New J. Phys.* **2013**, *15*, 075010.

23. Shiozaki, K.; Sato, M. Topology of crystalline insulators and superconductors. *Phys. Rev. B* **2014**, *90*, 165114.

24. Chiu, C.K.; Yao, H.; Ryu, S. Classification of topological insulators and superconductors in the presence of reflection symmetry. *Phys. Rev. B* **2013**, *88*, 075142.

25. Morimoto, T.; Furusaki, A. Topological classification with additional symmetries from Clifford algebras. *Phys. Rev. B* **2013**, *88*, 125129.

26. Ando, Y.; Fu, L. Topological Crystalline Insulators and Topological Superconductors: From Concepts to Materials. *Ann. Rev. Condens. Matter Phys.* **2015**, *6*, 361–381.

27. Chiu, C.K.; Teo, J.C.Y.; Schnyder, A.P.; Ryu, S. Classification of topological quantum matter with symmetries. *Rev. Mod. Phys.* **2016**, *88*, 035005.

28. Sigrist, M.; Ueda, K. Phenomenological theory of unconventional superconductivity. *Rev. Mod. Phys.* **1991**, *63*, 239–311.

29. Nomoto, T.; Hattori, K.; Ikeda, H. Classification of "multipole" superconductivity in multiorbital systems and its implications. *Phys. Rev. B* **2016**, *94*, 174513.

30. Sato, M.; Tanaka, Y.; Yada, K.; Yokoyama, T. Topology of Andreev bound states with flat dispersion. *Phys. Rev. B* **2011**, *83*, 224511.

31. Kobayashi, S.; Tanaka, Y.; Sato, M. Fragile surface zero-energy flat bands in three-dimensional chiral superconductors. *Phys. Rev. B* **2015**, *92*, 214514.

32. Sato, M. Topological odd-parity superconductors. *Phys. Rev. B* **2010**, *81*, 220504.

33. Izumida, W.; Okuyama, R.; Yamakage, A.; Saito, R. Angular momentum and topology in semiconducting single-wall carbon nanotubes. *Phys. Rev. B* **2016**, *93*, 195442.

34. Nakosai, S.; Tanaka, Y.; Nagaosa, N. Topological Superconductivity in Bilayer Rashba System. *Phys. Rev. Lett.* **2012**, *108*, 147003.

35. Yoshida, T.; Sigrist, M.; Yanase, Y. Pair-density wave states through spin-orbit coupling in multilayer superconductors. *Phys. Rev. B* **2012**, *86*, 134514.

36. Yoshida, T.; Sigrist, M.; Yanase, Y. Topological Crystalline Superconductivity in Locally Noncentrosymmetric Multilayer Superconductors. *Phys. Rev. Lett.* **2015**, *115*, 027001.

37. Kashiwaya, S.; Tanaka, Y. Tunnelling effects on surface bound states in unconventional superconductors. *Rep. Prog. Phys.* **2000**, *63*, 1641–1724.

38. Kobayashi, S.; Yanase, Y.; Sato, M. Topologically stable gapless phases in nonsymmorphic superconductors. *Phys. Rev. B* **2016**, *94*, 134512.